Received: 18 July 2017 | Accepted: 13 November 2017

DOI: 10.1002/rth2.12068

ORIGINAL ARTICLE

rpth research & practice in thrombosis & haemostasis

N-methyl-D-aspartate receptor mediated calcium influx supports in vitro differentiation of normal mouse megakaryocytes but proliferation of leukemic cell lines

Tania Kamal PhD[1] | Taryn N. Green MMedSci[1] | James I. Hearn MSc[1] | Emma C. Josefsson PhD[2,3] | Marie-Christine Morel-Kopp PhD[4,5] | Christopher M. Ward MBChB, PhD[4,5] | Matthew J. During MBChB, DSc[1,6] | Maggie L. Kalev-Zylinska MBChB, PhD[1,7]

[1]Department of Molecular Medicine & Pathology, University of Auckland, Auckland, New Zealand

[2]The Walter and Eliza Hall Institute of Medical Research, Parkville, Vic., Australia

[3]Department of Medical Biology, University of Melbourne, Melbourne, Vic., Australia

[4]Department of Haematology and Transfusion Medicine, Royal North Shore Hospital, Sydney, NSW, Australia

[5]Northern Blood Research Centre, Kolling Institute, University of Sydney, Sydney, NSW, Australia

[6]Departments of Molecular Virology, Immunology and Medical Genetics, Neuroscience and Neurological Surgery, Ohio State University, Columbus, OH, USA

[7]LabPlus Haematology, Auckland City Hospital, Auckland, New Zealand

Correspondence
Maggie L. Kalev-Zylinska, Department of Molecular Medicine & Pathology, University of Auckland, Auckland, New Zealand.
Email: m.kalev@auckland.ac.nz

Funding information
The Anne and David Norman Fellowship in Leukaemia and Lymphoma Research; Child Cancer Foundation, Grant/Award Number: 12/17; Lorenzo and Pamela Galli Charitable Trust; Leukaemia and Blood Cancer New Zealand; Genesis Oncology Trust

Abstract

Background: *N*-methyl-D-aspartate receptors (NMDARs) contribute calcium influx in megakaryocytic cells but their roles remain unclear; both pro- and anti-differentiating effects have been shown in different contexts.

Objectives: The aim of this study was to clarify NMDAR contribution to megakaryocytic differentiation in both normal and leukemic cells.

Methods: Meg-01, Set-2, and K-562 leukemic cell lines were differentiated using phorbol-12-myristate-13-acetate (PMA, 10 nmol L^{-1}) or valproic acid (VPA, 500 μmol L^{-1}). Normal megakaryocytes were grown from mouse marrow-derived hematopoietic progenitors (lineage-negative and CD41a-enriched) in the presence of thrombopoietin (30-40 nmol L^{-1}). Marrow explants were used to monitor proplatelet formation in the native bone marrow milieu. In all culture systems, NMDARs were inhibited using memantine and MK-801 (100 μmol L^{-1}); their effects compared against appropriate controls.

Results: The most striking observation from our studies was that NMDAR antagonists markedly inhibited proplatelet formation in all primary cultures employed. Proplatelets were either absent (in the presence of memantine) or short, broad and intertwined (with MK-801). Earlier steps of megakaryocytic differentiation (acquisition of CD41a and nuclear ploidy) were maintained, albeit reduced. In contrast, in leukemic Meg-01 cells, NMDAR antagonists inhibited differentiation in the presence of PMA and VPA but induced differentiation when applied by themselves.

Conclusions: NMDAR-mediated calcium influx is required for normal megakaryocytic differentiation, in particular proplatelet formation. However, in leukemic cells, the main NMDAR role is to inhibit differentiation, suggesting diversion of NMDAR activity to support leukemia growth. Further elucidation of the NMDAR and calcium pathways in megakaryocytic cells may suggest novel ways to modulate abnormal megakaryopoiesis.

KEYWORDS
calcium, cancer, glutamate, leukemia, megakaryocytes, *N*-methyl-D-aspartate receptor

Essentials

- Intracellular calcium pathways regulate megakaryopoiesis but details are unclear.
- We examined effects of NMDAR-mediated calcium influx on normal and leukemic cells in culture.
- NMDARs facilitated differentiation of normal but proliferation of leukemic megakaryocytes.
- NMDAR inhibitors induced differentiation of leukemic Meg-01 cells.

1 | INTRODUCTION

Megakaryocytes are unique hematopoietic cells. Their maturation involves unusual processes of polyploidisation[1] and proplatelet formation[2] regulated by dynamic changes in transcription factors such as GATA1, NF-E2, FLI1, and RUNX1.[3,4] Thrombopoietin (TPO) is the main humoral driver of megakaryopoiesis.[5,6] However, TPO does not regulate proplatelet formation,[7] a process requiring complex remodelling of cytoskeletal elements, including actin and microtubules.[8,9]

The contribution from intracellular calcium ions (Ca^{2+}) to megakaryocytic differentiation remains poorly understood but is an area of active research due to the discovery that 30% of patients with essential thrombocythaemia (ET) and primary myelofibrosis (PMF) harbor mutations in the *CALR* gene that encodes calreticulin.[10,11] Calreticulin is highly expressed in megakaryocytes and buffers Ca^{2+} in the endoplasmic reticulum (ER).[12,13] Mutations impair calreticulin ability to bind Ca^{2+},[14] which remodels Ca^{2+} pathways in mutated cells.[15] Megakaryocytes derived from patients with type 1 *CALR* mutations display stronger Ca^{2+} signals upon activation.[15] Peak values for both Ca^{2+} release from the ER stores and Store-Operated Ca^{2+} Entry (SOCE) are higher in these cells, compared with patients with type 2 *CALR* or *JAK2* V617F mutations, or in healthy subjects.

SOCE is initiated when Stromal Interaction Molecule 1 (STIM1) senses depletion of Ca^{2+} stores in the ER.[16] Uncontrolled SOCE can be pathogenic, as mice with the constitutively active *Stim1*^{Sax} mutation develop marrow fibrosis and splenomegaly, akin to human PMF.[17] Normal megakaryocytic differentiation requires fine regulation of SOCE.[18] TPO increases expression of molecules that facilitate SOCE, including those that release and refill intracellular Ca^{2+} stores.[19–22] Emerging data indicate that SOCE peaks during proplatelet formation and contributes to megakaryocyte adhesion and motility.[23]

The main pathway for SOCE in megakaryocytes is through Ca^{2+}-Release Activated Ca^{2+} channels formed by the ORAI1 proteins (in Greek mythology, Orai were the gatekeepers of heaven).[24] However, megakaryocytes also express other Ca^{2+} channels, including transient receptor potential cation (TRPC),[25] P2X,[26] P2Y,[27,28] nicotinic cholinergic[29] and *N*-methyl-D-aspartate (NMDA) receptors (NMDARs).[30,31] NMDARs are non-specific cation channels with high Ca^{2+} permeability activated by extracellular glutamate.[32] Although NMDARs have been best characterized in neurons, their functions in non-neuronal cells are being increasingly recognized, including in megakaryocytes.[30,31,33] Previous findings on the NMDAR function in megakaryocytic cells have been somewhat conflicting; both pro-[30,31] and anti-[33] differentiating effects have been shown in different cell types.

Motivated by the unclear role of megakaryocytic NMDARs and the clinical importance of Ca^{2+} pathways in ET and PMF, we examined NMDAR effects in multiple culture models of normal and leukemic megakaryocytes. Our results revealed that the impact of NMDAR activity on normal and leukemic cells is almost opposite, suggesting that leukemic cells remodel Ca^{2+} pathways to inhibit differentiation.

2 | MATERIALS AND METHODS

2.1 | Cultures of cell lines

Three human leukemia cell lines were used in this work: Meg-01, Set-2 (German Collection of Microorganisms and Cell Cultures [DSMZ], Braunschweig, Germany) and K-562 (American Type Culture Collection [ATCC], Manassas, VA). Cell lines were grown in supplemented RPMI-1640, as before.[33] To induce differentiation, cells were seeded in 6-well plates at 2×10^5 cells per well and cultured in the presence of phorbol-12-myristate-13-acetate (PMA; 10 or 25 nmol L^{-1}) for 3 days[34] or valproic acid (VPA; 500 μmol L^{-1}) for 7 days[35] (both from Sigma-Aldrich, Saint Louis, MO). L-glutamic acid (glutamate) and NMDA were used as NMDAR agonists (50-500 μmol L^{-1}); memantine (3,5-dimethyl-1-adamantanamine hydrochloride) and MK-801 ([+]-MK-801 hydrogen maleate) as NMDAR antagonists (25-100 μmol L^{-1}; Sigma-Aldrich). Cell viability was measured using 3-(4,5-dimethylthiazol-2-yl)-2,5-diphenyltetrazolium bromide (MTT) assay (Thermo-Fisher Scientific, Waltham, MA). Cell proliferation was quantified from the amount of 5-bromo-2′-deoxyuridine (BrdU) incorporated into synthesized DNA using Cell Proliferation ELISA kit (Roche-Applied Science, San Diego, CA).

2.2 | Isolation and cultures of primary mouse megakaryocytes

2.2.1 | Collection of mouse bone marrow

Bone marrow was collected from male C57BL/6 mice at 8 weeks of age, as approved by the Institutional Animal Ethics Committee (13/

R1245). Bone marrow was flushed out of bones with CATCH buffer (in mmol L^{-1}: 5.3 KCl, 0.44 KH_2PO_4, 137 NaCl, 4.17 $NaHCO_3$, 0.338 Na_2HPO_4, 5.56 glucose, 12.9 sodium citrate, 1.0 adenosine, 2.0 theophylline, 3% FCS [volume per volume; v/v], 3% BSA [weight per volume; w/v]). Disaggregated cells were passed through a 100 μm nylon mesh filter and centrifuged at 180 *g* for 10 minutes. Pelleted cells were re-suspended in CATCH buffer, overlaid over 1.050 g cm^{-3} Percoll (Sigma-Aldrich) and spun at 400 *g* for 30 minutes at room temperature (RT) with no brake. Cells were collected from the Percoll interphase, washed three times in CATCH buffer by centrifugation at 180 *g* for 10 minutes and re-suspended in CATCH buffer to 10^8 cells mL^{-1}.

2.2.2 | Cultures of CD41a-positive precursors

Megakaryocytic precursors were purified using Magnetic Activated Cell Sorting (MACS) kit with anti-PE microbeads (Miltenyi Biotech, Bergisch Gladbach, Germany). Briefly, cells were incubated with anti-CD41a-PE antibody diluted 1:20 for 15 minutes. Cells were washed, re-suspended in CATCH buffer and incubated with anti-PE microbeads. Unbound microbeads were removed by washing in CATCH buffer. Re-suspended cells were filtered through a pre-wet 100 μm nylon mesh and passed through equilibrated LS MiniMACS columns. Labelled cells were eluted, pelleted by centrifugation, re-suspended in PBS and cultured in StemSpan Serum-Free Expansion Medium II (SFEM II; StemCell Technologies, Vancouver, BC) containing 30 nmol L^{-1} TPO (Thermo-Fisher Scientific) for 3 days.

2.2.3 | Cultures of lineage-negative progenitors

Mouse bone marrow was obtained as above. Red cells were lysed in an ice-cold ACK buffer (in mmol L^{-1}: 155 NH_4CL, 10 $KHCO_3$, 0.1 EDTA) for 2 minutes and the lysis was stopped by adding an equal volume of PBS. Cells were passed through a 100 μm nylon mesh, spun at 300 *g* for 10 minutes and adjusted to a density of 2×10^7 cells per mL using MACS buffer (PBS containing 0.5% BSA, 5 mmol L^{-1} EDTA, 100 U mL^{-1} penicillin and 100 μg mL^{-1} streptomycin). Hematopoietic progenitors were isolated using a Lineage-depletion kit (Miltenyi) employing a cocktail of biotinylated antibodies targeting: CD5, CD45R (B220), CD11b, Gr-1 (Ly-6G/C), 7-4 and Ter-119, followed by anti-biotin microbeads. Cells were spun at 300 *g* for 10 minutes and passed through MS MiniMACS columns. Unlabeled (lineage-negative) cells were washed once in StemSpan SFEM II, plated at 0.5×10^6 cells per well in 6-well plates and cultured for 4 days in the presence of 40 nmol L^{-1} TPO.

2.2.4 | Cultures of bone marrow explants

Bone marrow explants were obtained and cultured as described.[36] Briefly, intact bone marrow cores were gently flushed out from mouse femurs using CATCH buffer, placed on Superfrost glass slides (Thermo-Fisher Scientific) flooded with CATCH buffer and cut into transverse sections of 0.5-1 mm thickness. Up to 10 sections were transferred to air-tight imaging chamber gaskets (CoverWell, Thermo-Fisher Scientific) filled with Tyrode's buffer (an isosmotic phosphate buffer pH 7.35 containing 0.1% sucrose [w/v], 0.35% human serum albumin [w/v], 2 mmol L^{-1} $CaCl_2$, 1 mmol L^{-1} $MgCl_2$ and 5% mouse serum [obtained in-house]). Explants were separated from each other and cultured at 37°C for 10 hours.

2.3 | Flow cytometry

2.3.1 | Cell lines

Suspended cells were collected from culture media by centrifugation at 100 *g*; adherent cells were lifted using 0.05% trypsin in 0.33 mmol L^{-1} EDTA. NMDAR subunits were tested using the following primary antibodies: anti-GluN1 (556308, BD Biosciences, San Jose, CA), anti-GluN2A (sc-9056, Santa Cruz Biotechnology, Santa Cruz, CA), anti-GluN2D (sc-10727, Santa Cruz), as before.[37] Anti- CD41a and CD61 antibodies (FITC- and PE-conjugated, respectively; BD Biosciences) were diluted 1:20 and incubated with cells for 20 minutes at RT. Ploidy was determined using propidium iodide (PI; 20 μg mL^{-1}; Thermo-Fisher Scientific).[33]

Platelet–like particles were examined as described.[35] Briefly, nucleated cells were collected by centrifugation at 100 *g* and the supernatant was re-spun at 1500 *g* (both for 10 minutes). Pelleted particles were re-suspended in ice-cold RPMI-1640 (supplemented with 10% FBS and 0.02% sodium azide) to 2×10^5 mL^{-1}. Anti- CD41a-FITC and CD61-PE antibodies were incubated as above.

2.3.2 | Primary cells

Megakaryocytes were enriched on a discontinuous density gradient (1.5-3%) of bovine serum albumin (BSA; Thermo-Fisher Scientific) followed by velocity sedimentation for 60 minutes at 1 *g*. Cells were collected from the bottom of the tube and suspended in StemSpan SFEM II media with 5% FBS. Expression of CD41a was tested as described above for cell lines. Nuclear ploidy was examined using Hoechst stain (10 μg mL^{-1}) incubated with cells at 37°C for 3 hours.

All flow cytometry data was acquired on a BD LSRII and analyzed using the following software: FACSDiva version 6.1.1 (BD Biosciences), FlowJo version 7.0 (TreeStar, Ashland, OR) and ModFit LT version 3.11 (for ploidy data; Verity Software House, Topsham, ME). Cells were gated based on forward and side scatter characteristics (FSC-A – SSC-A); cell doublets were excluded based on SSC-H – SSC-A and FSC-H – FSC-A (Figure S1). Platelet-like particles were examined using gates established by testing of human peripheral blood platelets (Figure S2).[37,38]

2.4 | Monitoring of intracellular Ca^{2+} responses

Meg-01 cells were seeded in RPMI-1640 glutamine-free medium at 2×10^4 cells per well in black, clear bottom 96-well plates coated with fibronectin (50 μg mL^{-1} in PBS) and grown for 3 days. Cytoplasmic

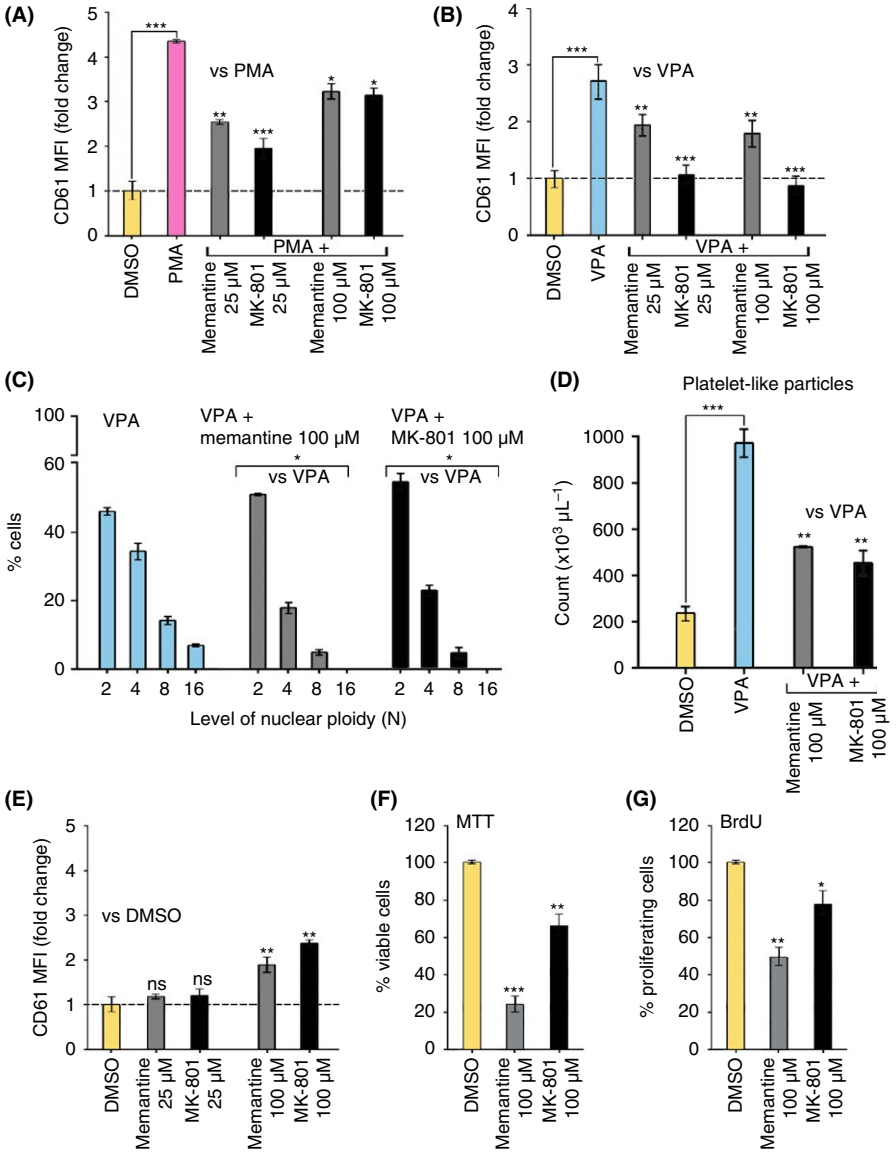

FIGURE 1 Effects of NMDAR antagonists on differentiation of Meg-01 cells. (A-D) Differentiation of Meg-01 cells was induced using 10 nmol L^{-1} PMA over 3 days (A) and 500 µmol L^{-1} VPA over 7 days. (B-D) Effects of NMDAR antagonists (memantine and MK-801; 25 and 100 µmol L^{-1}) were examined on CD61 expression (A, B), nuclear ploidy (C) and the production of platelet-like particles (D), all using flow cytometry. Bar graphs in A and B show a fold change in CD61 expression caused by memantine and MK-801 relative to PMA (in A) and VPA (in B). Flow cytometry gates on single Meg-01 cells are shown in Figure S1 and representative histogram examples of CD61 expression in Figure S4. (C) Effects of memantine and MK-801 on nuclear ploidy in the presence of VPA; 2, 4, 8, and 16 N indicate classes of nuclear ploidy. (D) Enumeration of CD61-positive platelet-like particles produced by Meg-01 cells in the presence of VPA, without and with NMDAR antagonists. Flow cytometry gates are shown in Figure S2 and representative histogram examples of CD61 expression in Figure S6. (E-G) Effects of NMDAR antagonists on spontaneous differentiation of Meg-01 cells (with no PMA or VPA added). Bars show effects of memantine and MK-801 on: CD61 expression (E; tested by flow cytometry), cell numbers (F; using MTT assay) and cell proliferation (G; from BrdU incorporation). All graphed data are mean ± SEM obtained from three independent experiments. Statistical significance is shown (*$P < .05$; **$P < .01$; ***$P < .001$). Data were analyzed by one-way ANOVA with Dunnett's post-hoc, except for ploidy that was analyzed by two-way ANOVA with Bonferroni correction for multiple comparisons. BrdU, 5-bromo-2′-deoxyuridine; DMSO, dimethyl sulfoxide; MFI, Mean Fluorescence Intensity; MTT, 3-(4,5-dimethylthiazol-2-yl)-2,5-diphenyltetrazolium bromide; ns, non-significant; PI, Propidium Iodide; PMA, phorbol-12-myristate-13-acetate; VPA, valproic acid

Ca^{2+} levels were monitored using Fluo-4-AM (acetoxymethyl ester) and a Fluo-4-NW Calcium Assay kit (Thermo-Fisher Scientific) according to manufacturer's instructions; details were recently described.[39] The imaging buffer contained 2.3 mmol L^{-1} $CaCl_2$ and 1% FBS. The fluorescence signal was read from the bottom of the plate on an EnSpire 2300 Multimode Plate Reader (Perkin-Elmer, Waltham, MA) with an excitation wavelength of 494 nm and emission at 516 nm. Baseline fluorescence was recorded for 10 seconds, after which the activator was added and imaging continued until 300 seconds. NMDAR antagonists were aliquoted into wells just before adding the activator. Fold

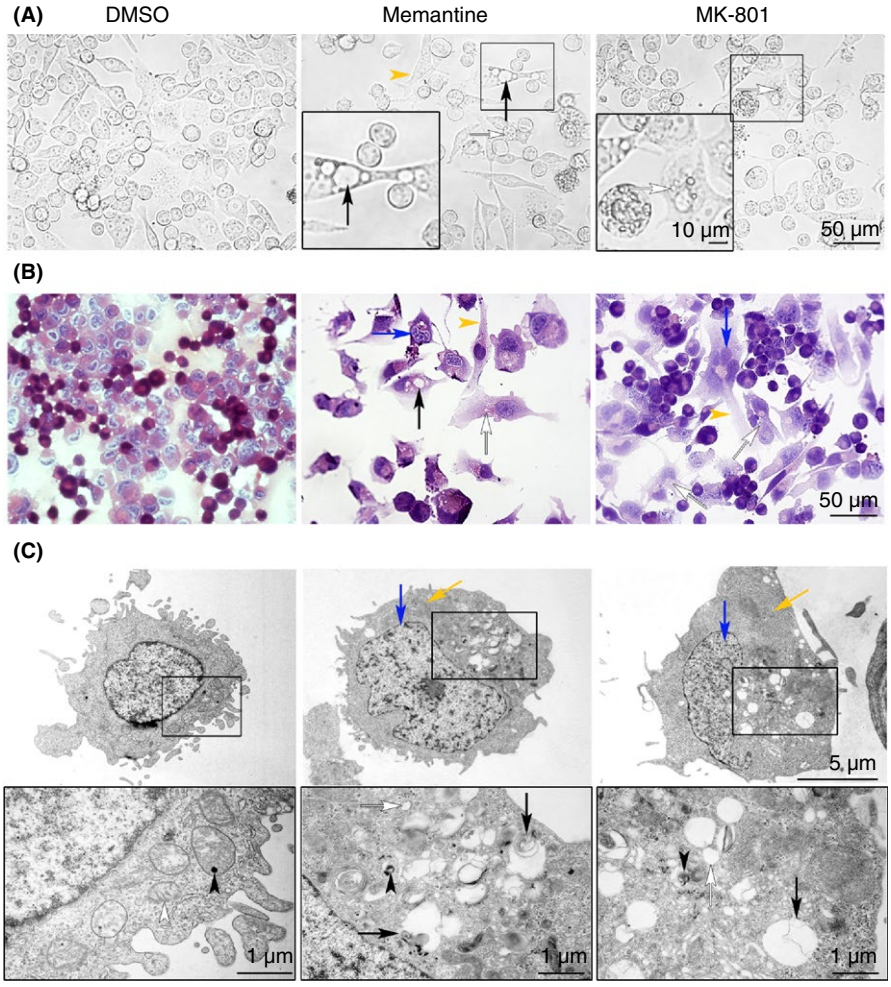

FIGURE 2 Effects of NMDAR antagonists on the morphology of Meg-01 cells. Meg-01 cells were cultured for 3 days in the presence of DMSO (0.1%; negative control), memantine and MK-801 (both at 100 µmol L^{-1}). (A) Live cells were imaged under phase contrast; fixed cells after Giemsa staining (B) and under transmission electron microscopy (TEM; C). TEM sections were examined in a Tecnai G2 Spirit Twin microscope (FEI Company, Hillsboro, OR) equipped with a Morada camera (Olympus-Soft Imaging Solutions, Singapore). Other images were taken using Eclipse microscopes (Nikon, Tokyo, Japan), inverted (A) or upright (B). All images are representative of at least three independent experiments. Examples of the following morphological features are pointed to: large and small cytoplasmic vacuoles (black and white arrows, respectively); multi-lobulated nuclei (blue arrows); an increased amount of cytoplasm with cytoplasmic extensions (yellow arrows and arrowheads, respectively); dense granules (black arrowheads) and mitochondria (white arrowhead, evident only under control conditions). Scale bars are shown

changes in Ca^{2+} levels were calculated relative to a buffer or diluent controls using average fluorescence values recorded at baseline and 40 s after the addition of modulators, when Ca^{2+} responses were maximal.

2.5 | Glutamate concentrations

Meg-01 cells were seeded in 6-well plates at 2×10^5 cells per well and grown in the presence or absence of 500 µmol L^{-1} VPA for 7 days. On days 0, 4, and 7, media samples were collected and stored at −80°C until testing. Glutamate concentrations were determined in batched media using an Amplex Red Glutamic Acid/Glutamate Oxidase Assay kit (Thermo-Fisher Scientific) according to manufacturer's instructions, with some modifications as we recently described.[39] Fluorescence was read on an EnSpire 2300 plate reader using excitation of 530 nm and emission at 590 nm.

2.6 | Molecular work

RNA isolation, cDNA synthesis and reverse transcription (RT) PCR were performed as before.[37] Primer sequences and PCR conditions were provided in Kamal et al. and Kalev-Zylinska et al.[33,37]

2.7 | Cell ultrastructure and immunofluorescence

Our method for transmission electron microscopy (TEM) was previously described.[37] Filamentous actin (F-actin) was visualized using Alexa Fluor 488 Phalloidin (Thermo-Fisher Scientific).[40]

2.8 | Statistical analysis

Statistical analysis was conducted using GraphPad Prism 5.0 (San Diego, CA) software for Windows. Data are shown as mean ± standard error of the mean (SEM). Mean differences between groups were analyzed by one-way or two-way analysis of variance (ANOVA), as indicated with Dunnett's post-hoc. Bonferroni correction was applied to multiple comparisons. *P* values less than .05 were considered statistically significant.

3 | RESULTS

3.1 | NMDARs facilitate PMA- and VPA-induced differentiation of Meg-01 cells

NMDAR involvement in megakaryocytic differentiation was first examined using a traditional PMA-driven model of cell line differentiation[34]

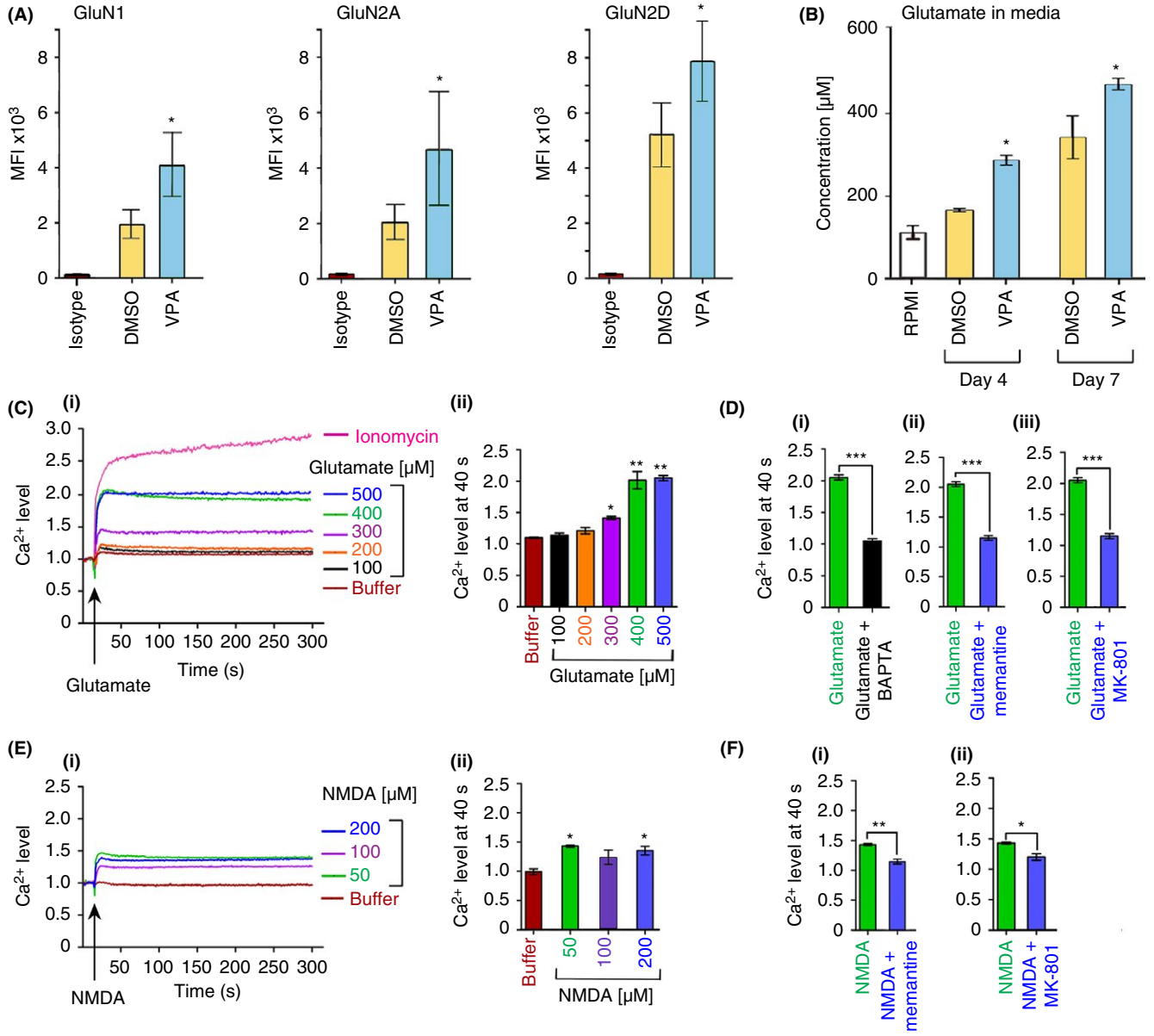

FIGURE 3 NMDAR expression, glutamate release and NMDAR-mediated Ca^{2+} responses in differentiated Meg-01 cells. (A, B) Meg-01 cells were cultured for 7 days in the presence of 500 μmol L^{-1} VPA or 0.1% DMSO control, after which surface expression of the NMDAR subunits and glutamate release were measured. Bar graphs in A demonstrate MFI readings (mean ± SEM) for the expression of GluN1, GluN2A and GluN2D on the surface of Meg-01 cells, as determined by flow cytometry in three independent experiments. Bar graphs in B demonstrate glutamate concentrations in media in which Meg-01 cells were cultured for 4 or 7 days, as indicated. Each bar represents mean ± SEM from three independent experiments for which each media sample was tested in triplicate. RPMI is a stock media sample used for plating. (C-F) NMDAR-mediated intracellular Ca^{2+} responses in differentiated Meg-01 cells. Cells were loaded with Fluo-4-AM and intracellular Ca^{2+} levels recorded on a plate reader in response to the following agonists: glutamate 100-500 μmol L^{-1} (in C) and 400 μmol/L (in D); NMDA – 50-200 μmol L^{-1} (in E) and 50 μmol L^{-1} (in F). Line graphs in C.i and E.i show mean relative levels of intracellular Ca^{2+} recorded over 300 seconds calculated from three independent experiments for each condition. Fold change was determined from the average fluorescence values acquired between the 1 and 16 seconds time points before the addition of activators. The bar graphs in C.ii, D.i-iii, E.ii, and F.i-ii show mean ± SEM of relative Ca^{2+} levels for the response during the early plateau at 40 seconds under the conditions indicated. The extracellular buffer contained 2.3 mmol L^{-1} $CaCl_2$ in all experiments. Error bars are not shown in line graphs for clarity but are displayed for all bar graphs. Ionomycin (5 μg mL^{-1}) was used as positive control and buffer or diluent as negative controls. Each experiment was repeated at least three times using cells of different passages. Within each experiment, measurements were taken from triplicate wells. Statistical significance is shown (*P < .05; **P < .01; ***P < .001; one-way ANOVA with Dunnett's post-hoc). MFI, mean fluorescence intensity; ns, non-significant; VPA, valproic acid

(Figure S3). Three human cell lines, Meg-01, K-562, and Set-2, were tested for differentiation responses to PMA over 3 days, which identified that Meg-01 cells differentiated best. While K-562 and Set-2 cells remained small, round and in suspension (data not shown), Meg-01 cells displayed obvious features of megakaryocytic differentiation, including large, adherent morphology and proplatelet-like cytoplasmic

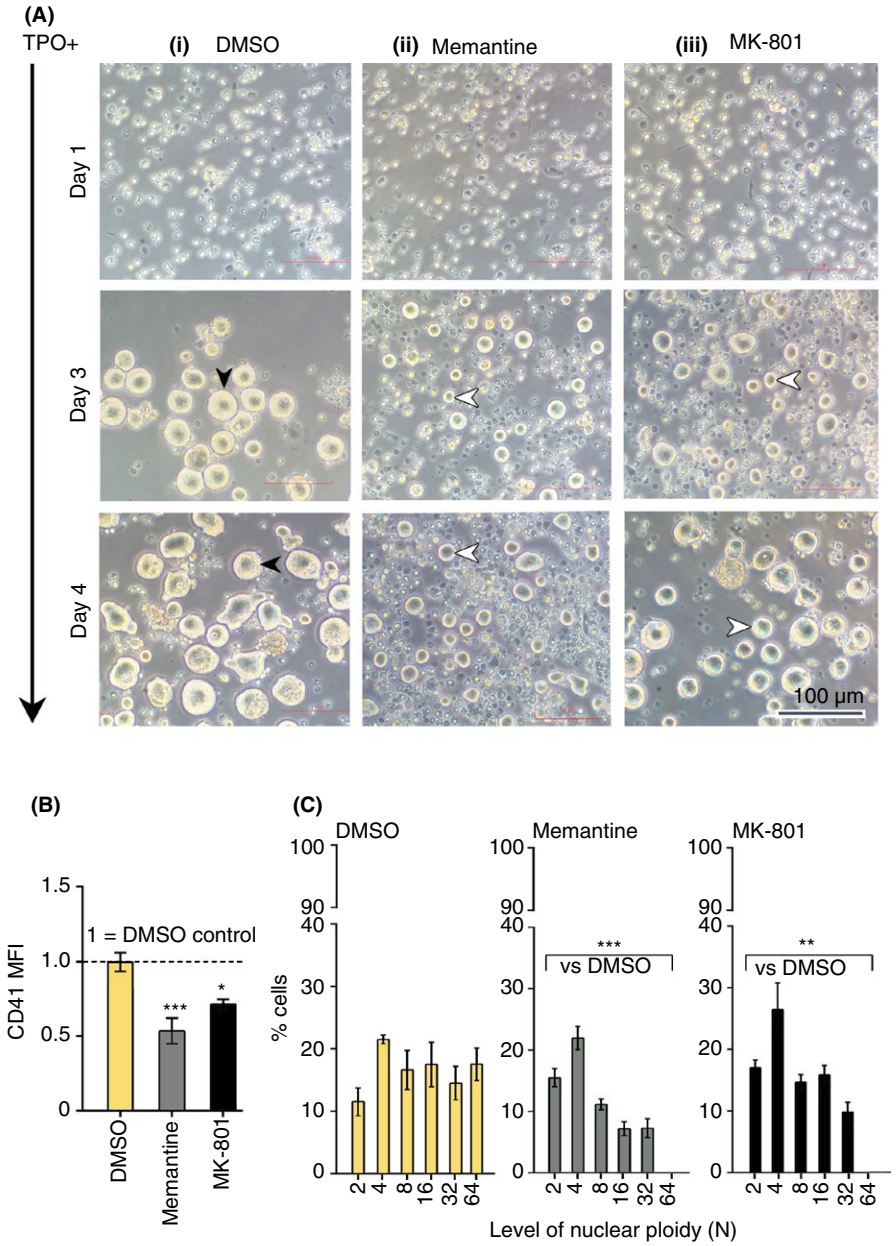

FIGURE 4 Effects of NMDAR antagonists on megakaryocytic differentiation from hematopoietic progenitors. Lineage-negative progenitors were isolated from mouse marrow and cultured for 4 days in SFEM II media supplemented with 40 nmol L^{-1} thrombopoietin. Memantine and MK-801 were added (both at 100 µmol L^{-1}) or 0.1% DMSO control, as indicated. (A) Representative phase-contrast photomicrographs show the morphology of live cells on days 1, 3, and 4 of lineage-negative cultures from three independent experiments. Cell morphology has not changed much on day 2 (hence, not shown). In the presence of DMSO (A.i), large, polylobated megakaryocytes dominated on days 3 and 4 (examples are pointed to by black arrowheads). In comparison, megakaryocytic progenitors cultured in the presence of NMDAR antagonists (A.ii-A.iii), in particular memantine were smaller (as those pointed to by white arrowheads). Scale bar, 100 µm for all. (B, C) Bar graphs showing fold change in the expression of CD41a (in B) and nuclear ploidy (in C) for megakaryocytic cells enriched on BSA gradient at the end of lineage-negative cultures. Classes of nuclear ploidy are indicated as 2, 4, 8, 16, 32 and 64 N. Data was graphed as mean ± SEM from three independent experiments. Statistical significance is shown (*P < .05; **P < .01; ***P < .001). The immunophenotypic data was analyzed by one-way ANOVA with Dunnett's post-hoc, ploidy by two-way ANOVA. MFI, Mean Fluorescence Intensity; ns, non-significant

extensions (Figure S3A). In keeping with these appearances, cell marker studies revealed increased expression of CD41a and CD61 (Figure S3B). Signs of differentiation were stronger when PMA was applied at 25 nmol L^{-1} but cell damage also developed, hence subsequent studies used 10 nmol L^{-1} PMA to provide a model in which to determine NMDAR involvement in megakaryocytic differentiation. When added to 10 nmol L^{-1} PMA, memantine and MK-801 (25 and 100 µmol L^{-1}) attenuated PMA-driven expression of CD41a and CD61, suggesting NMDAR involvement in megakaryocytic differentiation (Figures 1A and S4A; data for CD41a not shown).

PMA acts by activating protein kinase C (PKC)[41] and PKC phosphorylates and activates NMDAR proteins directly.[42] We thus asked

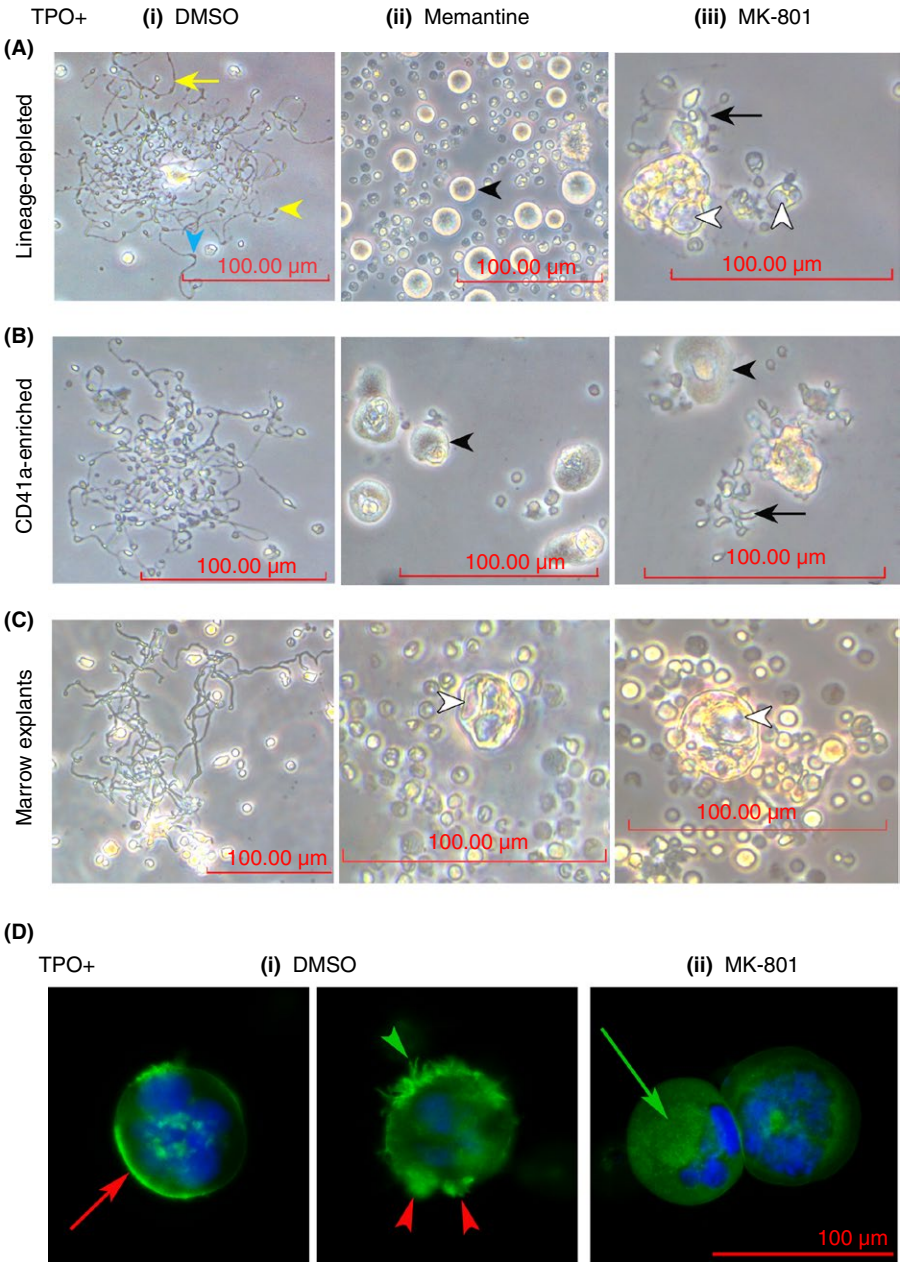

FIGURE 5 Proplatelet formation in mouse megakaryocytes cultured in the presence of NMDAR antagonists. (A) Proplatelets were observed in cultures of: (A) lineage-negative bone marrow progenitors; (B) CD41a-enriched megakaryocytic precursors; (C) bone marrow explants. Memantine and MK-801 were used at 100 µmol L^{-1} or 0.1% DMSO control, as indicated. Morphology of live cells was monitored using phase-contrast. The following features of normal proplatelets are indicated in A.i: thin branched proplatelet shafts (yellow arrows), proplatelet buds (yellow arrowheads) and intermediate swellings (blue arrowheads). In all culture types, when memantine was present, most megakaryocytes remained spherical and proplatelets did not form (black arrowheads). In the presence of MK-801, rare proplatelets were seen but these remained short and disorganized (black arrows). In addition, large cytoplasmic vacuoles were seen in cultures containing NMDAR antagonists (white arrowheads). (D) F-actin was stained in megakaryocytic cells generated in lineage-negative cultures and enriched on Percoll gradient. Cells were fixed with 4% paraformaldehyde, permeabilized with 0.1% Triton-X, stained using Alexa Fluor 488 Phalloidin and counter-stained with Hoechst 33258. (D.i) The following signs of actin reorganization are pointed to in the presence of DMSO: peripheral enhancement (red arrow), focal complex formation (red arrowheads) and peripheral fibre extensions (green arrowhead). (D.ii) Staining of actin in megakaryocytes that matured in the presence of MK-801 showed no obvious features of polymerization (green arrow highlights diffuse intracellular staining). Images are representative of three independent experiments. Scale bars, 100 µm for all

whether NMDAR contribution to PMA effects was a simple consequence of PKC overactivation specific to this model, and not a true reflection of NMDAR involvement in megakaryocytic differentiation. We employed VPA as an alternative pro-differentiating chemical that works primarily by modulating transcription.[43] VPA (500 µmol L^{-1}) induced potent differentiation of Meg-01 cells with little toxicity (Figure S5). Despite its different mechanism of action, NMDAR antagonists inhibited VPA effects. Similar to what we found in the presence

TABLE 1 Effects of NMDAR antagonists on proplatelet formation

	Numbers of megakaryocytes forming proplatelets			
Culture type	DMSO	Memantine	MK-801	*P*-value
Lineage-negative progenitors[a]	12 ± 5	0	3 ± 1	<.01
CD41a-enriched precursors[b]	6 ± 2	0	2 ± 1	<.05
Bone marrow explants[c]	28 ± 1	0	2 ± 1	<.001

Numbers of megakaryocytes producing proplatelets were counted at completion of each culture type. Counts are mean ± SEM from three independent experiments for each culture type.
[a]Counts are per well in 6-well plates.
[b]Counts are per well in 24-well plates.
[c]Counts are per chamber containing eight explants. *P*-values indicate a difference between the modulator and the DMSO control calculated by one-way ANOVA with Dunnett's post-hoc.

of PMA, memantine and MK-801 (25 and 100 μmol L^{-1}) reduced VPA-driven expression of CD61, nuclear ploidy and the release of platelet-like particles (Figures 1B-D, S4B and S6). Taken together, our results argued that active NMDARs were required for chemically-induced differentiation of Meg-01 cells.

3.2 | Paradoxically, NMDARs increase proliferation of Meg-01 cells

Unexpectedly, when used without PMA and VPA, NMDAR inhibitors increased differentiation of Meg-01 cells. This was evidenced by the enhanced expression of CD61, lower cell numbers and less proliferation when cells were cultured with 100 μmol L^{-1} memantine and MK-801, compared with DMSO-treated controls (Figure 1E-G). Morphologically, when NMDAR inhibitors were present, cells became larger, acquired nuclear lobulation and cytoplasmic extensions. In addition, distinct cytoplasmic vacuoles developed, some of which were quite large, others small and located mostly in the Golgi and perinuclear regions (Figure 2A, B). TEM analysis suggested that these vacuoles represented endolysosomes or dilated ER; other ultrastructural changes observed in the presence of NMDAR antagonists included atypical appearances of dense granules and the paucity of mitochondria (Figure 2C).

3.3 | NMDAR functionality increases in differentiated Meg-01 cells

Intrigued by the evidence that NMDARs modulate differentiation of Meg-01 cells, we sought a link between the state of cell differentiation and the NMDAR activity.

Meg-01 cells were differentiated using VPA over 7 days (as described above) followed by testing of NMDAR expression and glutamate release (Figure 3A, B). Surface expression of the main three NMDAR subunits, GluN1, GluN2A, and GluN2D was examined by flow cytometry and glutamate content was measured in media samples collected on days 0, 4, and 7. This found that VPA treated Meg-01 cells carried higher levels of surface GluN1, GluN2A and GluN2D (Figure 3A) and released more glutamate (Figure 3B), implying a link between megakaryocytic differentiation and the glutamate-NMDAR axis.

The NMDAR-mediated Ca^{2+} fluxes were then examined in populations of differentiated Meg-01 cells (Figure 3C-F). Adherent cells were washed, loaded with Fluo4-AM and Ca^{2+} fluxes recorded in a buffer containing 2.3 mmol L^{-1} $CaCl_2$ using a high-throughput plate reader. Glutamate (100-500 μmol L^{-1}) and NMDA (50-200 μmol L^{-1}) caused rapid rises in cytoplasmic Ca^2 levels that stabilized within 30-50 seconds (Figure 3C, E). Glutamate induced increasing Ca^{2+} responses from 100 to 500 μmol L^{-1} in a dose-dependent manner; NMDA effects were weaker but supported specific engagement of the NMDAR. Chelation of extracellular Ca^{2+} with 5 mmol L^{-1} BAPTA inhibited NMDAR-mediated Ca^{2+} rises (Figure 3D.i), indicating a requirement for Ca^{2+} entry in the glutamate response. Memantine and MK-801 also attenuated Ca^{2+} fluxes (Figure 3D.ii-iii, F.i-ii), providing further support for the NMDAR engagement in these responses.

3.4 | NMDARs facilitate proplatelet formation by mouse megakaryocytes

Motivated by the findings that megakaryocytic NMDARs are functional and impact differentiation of Meg-01 cells, we proceeded to examine NMDAR contribution in normal mouse megakaryocytes.

Lineage-negative progenitors were isolated from mouse bone marrow and cultured for 4 days in SFEM II media containing 40 nmol L^{-1} TPO. Over time, control cells increased in size, consistent with megakaryocytic differentiation (Figure 4A.i). The addition of memantine and MK-801 restricted cell size increases, suggesting NMDAR involvement in TPO-driven megakaryocytic differentiation (Figure 4A.ii-iii). At the end of cultures, larger cells were enriched on BSA gradient and their state of differentiation examined by flow cytometry. Cells cultured in the presence of memantine and MK-801 showed less expression of CD41a and lower nuclear ploidy than cells treated with TPO alone (Figure 4B, C), supporting NMDAR involvement in early megakaryocytic differentiation. In comparison, without TPO, NMDAR antagonists were insufficient to induce megakaryocytic differentiation of lineage-negative progenitors (Figure S7).

Our lineage-negative cultures produced proplatelets on day 5. Control proplatelets had long, thin and branched shafts, buds and intermediate swellings connected by thin cytoplasmic bridges, as

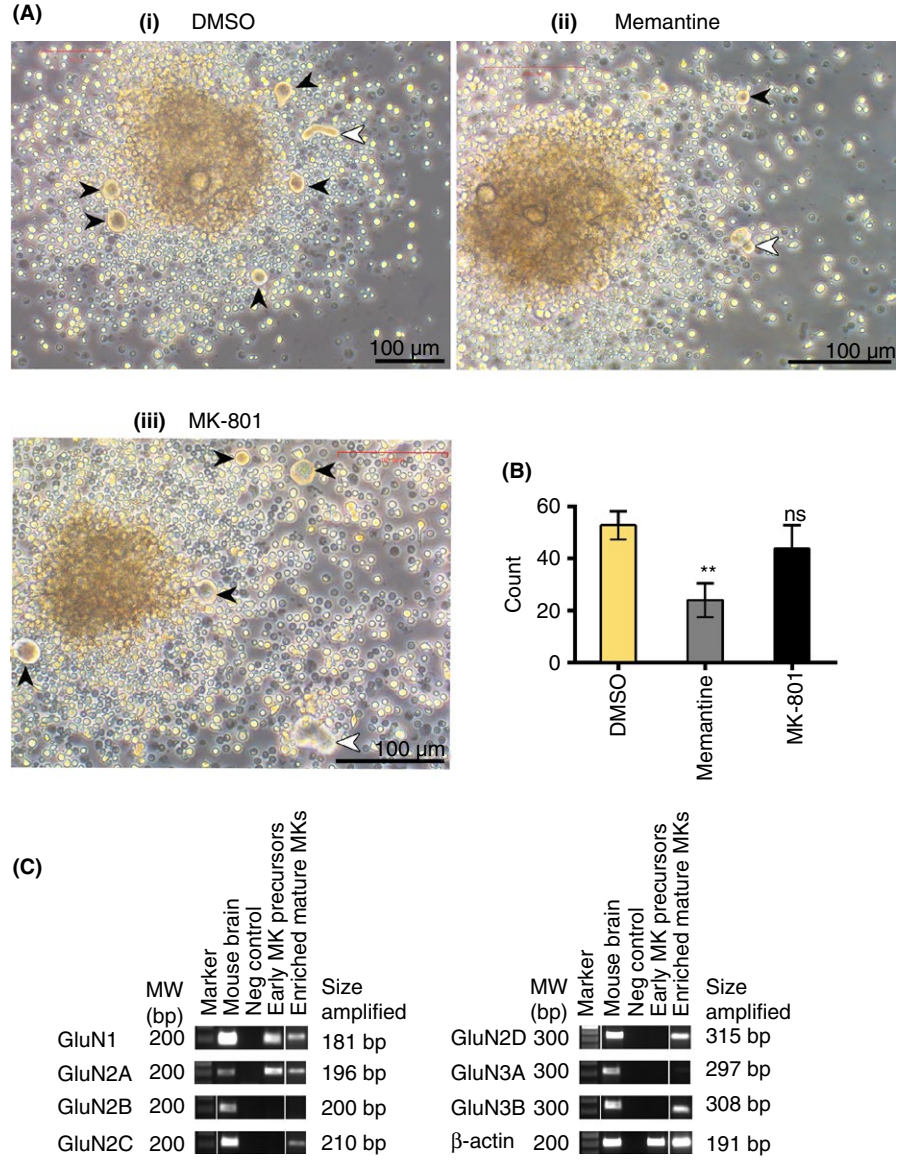

FIGURE 6 Bone marrow explant cultures and NMDAR expression in cultured cells. (A) Bone marrow explants were isolated from mice femurs and cultured at 37°C in gaskets containing Tyrode's buffer supplemented with 5% mouse serum. Memantine and MK-801 were added at 100 µmol L^{-1}; control cultures contained 0.1% DMSO. Phase-contrast photomicrographs are shown taken at 3 hours into cultures. Three independent experiments were performed for each condition, representative images are shown. Arrowheads point to megakaryocytes that migrated out of explants; those indicated by white arrowheads already produced cytoplasmic protrusions. Scale bars, 100 µm. (B) Bars indicate numbers of megakaryocytes that migrated out of explants. (C) RT-PCR results demonstrate expression patterns for all NMDAR subunits in early and late mouse megakaryocytes. Early megakaryocytes were a pool of precursors generated in the presence of thrombopoietin from lineage-negative progenitors. Mature megakaryocytes were isolated from mouse bone marrow on Percoll gradient, followed by immunomagnetic selection of CD41a-expressing cells. All PCR reactions were performed in triplicates using 2-3 independent biological samples

previously described[2] (Figure 5A.i). Memantine and MK-801 markedly reduced proplatelet formation in these cultures (Table 1). In the presence of memantine, proplatelets were virtually not seen; and in the presence of MK-801, proplatelets were rare, short and distorted, including looping forms. In addition, large cytoplasmic vacuoles also developed within the cell bodies of megakaryocytes (Figures 5A.ii-iii and S8).

The impact of memantine and MK-801 on proplatelet formation was so striking that we sought confirmation in cultures of CD41a-enriched precursors. CD41a-positive cells were cultured for 3 days in the presence of 30 nmol L^{-1} of TPO (Figure 5B). Similar to their effects in lineage-negative cultures, memantine abrogated proplatelet formation from CD41a-positive precursors (Table 1; Figure 5B.ii). Rare proplatelet-bearing megakaryocytes were seen in the presence of MK-801, but these were stunted without proper proplatelet branching seen in controls (Table 1; Figures 5B.iii and S8).

Bone marrow explants were used next to confirm NMDAR effects in the native bone marrow milieu (with no exogenous TPO added; Figure 5C). Mouse femurs were dissected, bone marrow cores flushed out, cut into slices, and cultured in hypoxic chambers over poly-L-lysine-coated slides. Similar to other cultures, no proplatelets arose from explants exposed to memantine and cytoplasmic vacuoles were frequent (Table 1; Figure 5C.i). Rare proplatelets that formed in the presence of MK-801 were short and contorted (Figure S8).

We hypothesized that abnormal proplatelet formation in the presence of memantine and MK-801 reflected a defect in the cytoskeleton reorganization. Previous work showed that extracellular Ca^{2+} entry regulates actin polymerization,[23] so we stained cells with phalloidin to visualize actin fibers (Figures 5D and S9). Control megakaryocytes displayed obvious signs of actin reorganization, including peripheral enhancement of staining, focal complex formation, and peripherally extending filaments (Figure 5D.i). In contrast, cells cultured in the presence of MK-801 showed little signs of actin reorganization (Figures 5D.ii and S9), implying NMDAR involvement in this process.

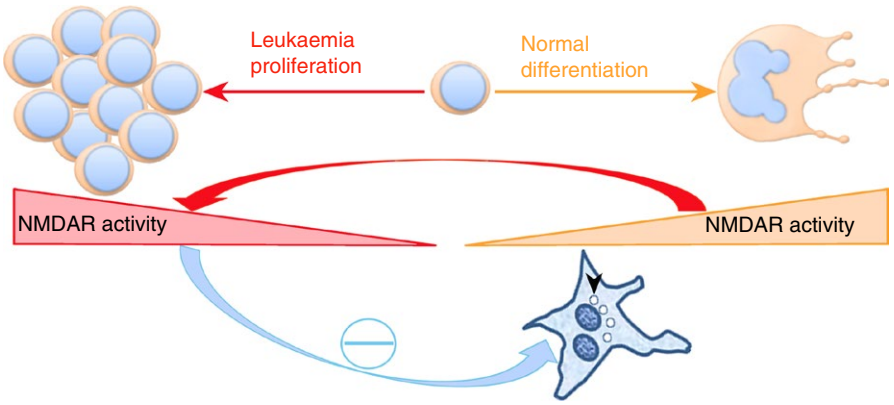

FIGURE 7 Schematic highlighting NMDAR effects in normal and leukemic megakaryocytes. In normal megakaryocytes, NMDAR activity increases upon cell differentiation and supports proplatelet formation (orange shapes). In contrast, in leukemic Meg-01 cells NMDAR activity inhibits differentiation and increases proliferation (red shapes). NMDAR antagonists, including memantine, which is an existing neurological drug, induces partial differentiation of Meg-01 cells (blue arrow) associated with distinct cytoplasmic vacuoles (black arrowhead)

Further analysis of bone marrow explant cultures raised a possibility that NMDARs contribute to megakaryocyte migration. Memantine reduced numbers of megakaryocytes migrating out of explants ($P = .03$; Figure 6A, B). However, this was not found for MK-801; therefore, firm conclusions could not be drawn and further work is required to investigate NMDAR involvement in cell migration.

Finally, we confirmed that primary megakaryocytic cells we modulated in culture carried NMDAR subunits. GluN1 and GluN2A were expressed in early megakaryocytic precursors derived from lineage-negative progenitors (Figure 6C). Other NMDAR subunits, except for GluN2B and GluN3A, were also expressed in enriched mature megakaryocytes (Figure 6C). One can speculate that different NMDAR subunits may be influencing distinct NMDAR effects in early and late megakaryocytes.

4 | DISCUSSION

This study demonstrates that NMDAR-mediated Ca^{2+} influx is required for in vitro differentiation of normal mouse megakaryocytes, in particular for proplatelet formation. This is in contrast to the predominant anti-differentiating effects of active NMDARs in untreated Meg-01 cells. We found that upon VPA treatment, NMDAR expression and glutamate release increased in Meg-01 cells, compared with controls. In keeping with this, inhibiting NMDAR function with standard antagonists (memantine and MK-801) reduced pro-differentiating effects of PMA and VPA. However, Meg-01 cells not exposed to PMA or VPA but treated with NMDAR antagonists also exhibited differentiation. In comparison, in normal, immature mouse megakaryocytes (derived from lineage-depleted and CD41a-enriched progenitors), inhibition of NMDAR function reduced acquisition of CD41a and nuclear ploidy. Further, in mature mouse megakaryocytes (derived from bone marrow explants and ex-culture), the presence of memantine and MK-801 inhibited proplatelet formation.

The seminal evidence that NMDARs are involved in megakaryocytic differentiation was published in 2003,[31] but there have been no further reports. The 2003 publication described that human megakaryocytes grown in the presence of MK-801 were smaller and produced no proplatelets, compared with control cells grown without MK-801.[31] Results from our study are in agreement and contribute a more detailed picture of the NMDAR involvement in megakaryocytic differentiation.

Intriguingly, the proplatelet defect resulting from NMDAR inhibition resembled those previously reported in the presence of cytoskeletal disrupting agents. Nocodazole, that disrupts microtubules, prevents elaboration of proplatelets; cytochalasin B, an inhibitor of actin polymerization, reduces proplatelet branching.[2,44] Our results suggest a link between NMDAR function and the cell cytoskeleton in megakaryocytes, as it is also known to occur in neurons. NMDARs interact with actin and microtubules to physically re-shape neurons in response to neuronal firing,[45,46] including formation of cytoplasmic filopodia and dendritic spines.[47,48] There are also other examples of a similar link in non-neuronal cells. In renal podocytes, NMDARs re-shape cellular foot processes that regulate glomerular filtration.[49] To link with the cytoskeletal elements, neuronal NMDARs require post-synaptic density (PSD) proteins such as PSD-95 and Yotiao[32]; both of these are expressed in megakaryocytes[31]; hence these cells contain the molecules to support such interactions. We speculate that NMDAR effects on earlier stages of megakaryocytic differentiation (acquisition of CD41a and nuclear ploidy) involve other downstream mediators, in particular Nuclear Factor of Activated T-cells (NFAT).[50] The calcineurin-NFAT pathway responds to subtle changes in intracellular Ca^{2+} levels to inhibit progenitor proliferation and increase megakaryocytic differentiation[51]; therefore, NFAT regulation by NMDAR-mediated Ca^{2+} influx warrants testing in megakaryocytes.

This study has a number of limitations. Our observations were obtained in cell culture, and culture media contain ample amounts of glutamate: 136 μmol L^{-1} in RPMI-1640 and 510 μmol L^{-1} in SFEM II—manufacturer's specifications were confirmed (Figure 3 and in[39]). In contrast, glutamate signals in vivo are likely to be spatially restricted

and dynamically regulated. Previous work demonstrated that glutamate is released from megakaryocytes[52] and osteoblasts.[53] We did not repeat these experiments but acknowledge that further testing of glutamate release would be of interest, in particular in the native bone marrow environment. The mechanism through which NMDAR activity regulates megakaryocyte maturation requires elucidation. Our results suggest that in late megakaryocytes, NMDAR-mediated Ca^{2+} entry impacts reorganization of the cell cytoskeleton, but more precise characterization will need to follow. In comparison, other downstream targets may be contributing in early megakaryocytes; we suggest examination of a link with calcineurin-NFAT pathway may be informative. Possible involvement of NMDARs in megakaryocyte migration requires verification. Future studies should include trans-well migration assays that incorporate both glutamate modulators and components of extracellular matrix not present in our cultures. We accept that off-target effects, including non-specific perturbations in Ca^{2+} homeostasis cannot be excluded for chemical modulators; hence, genetic confirmation of our findings is being pursued. Meg-01 cells are not truly megakaryocytic so the differences in Ca^{2+} effects between Meg-01 and primary megakaryocytic cells could be a feature of the Meg-01 cell line; studies in other leukemia models and patient cells will need to follow.

Based on previous and our data, we expect that the following sequence of events applies in normal megakaryocytes. Engagement of surface receptors by ligands or matrix components activates phospholipase C (PLC). PLC generates inositol 1,4,5-triphosphate (IP3) that binds to IP3 receptors on the ER leading to the release of Ca^{2+} from its stores. The emptying of the ER stores triggers SOCE that occurs mostly through the ORAI1 channels activated by STIM1.[18,24] We suggest that NMDARs contribute to SOCE, which in early progenitors curtails proliferation while later in differentiation, drives proplatelet formation. In contrast to pro-differentiating effects in normal megakaryocytes, NMDAR pathways in leukemic cells inhibit differentiation and increase proliferation (Figure 7). Intriguingly, inhibition of NMDAR activity in leukemic cells using modulators such as memantine reverses the hijacking effect and induces differentiation, suggesting an anti-leukemic strategy for further testing.

In summary, our results indicate that active NMDARs are required for in vitro differentiation of normal mouse megakaryocytes, in particular proplatelet formation. However, in Meg-01 cells, NMDAR pathways are involved in de-differentiation and proliferation. The pro-differentiating effect of NMDAR antagonists in leukemic Meg-01 cells suggests a diversion of Ca^{2+} pathways towards proliferation, also reported in other cancers.[54,55] Our further studies will examine samples from patients with ET, PMF, and megakaryoblastic leukemia to closer characterize Ca^{2+} remodelling in disease.

AUTHOR CONTRIBUTIONS

T. Kamal performed experiments, analyzed data and drafted the manuscript. T. N. Green and J. I. Hearn provided technical support. E. C. Josefsson and M-C. Morel-Kopp helped with methodology and experimental design. C. M. Ward and M. J. During provided mentorship and advice. M. L. Kalev-Zylinska designed the study, supervised research, helped interpret data and wrote the paper.

RELATIONSHIP DISCLOSURES

T. Kamal received The Anne and David Norman Fellowship in Leukaemia and Lymphoma Research. Working expenses were funded by Child Cancer Foundation (project 12/17), Leukaemia & Blood Cancer New Zealand and Genesis Oncology Trust. E. C. Josefsson is the recipient of a fellowship from the Lorenzo and Pamela Galli Charitable Trust. Yohanes Nursalim performed electron microscopy guided by Jacqueline Ross and Hilary Holloway (Biomedical Imaging Research Unit). Stephen Edgar helped with flow cytometry and Dr Sue McGlashan advised on the use of phalloidin. We are grateful to Dr Elizabeth C. Ledgerwood for helpful discussions and comments on the manuscript.

ORCID

James I. Hearn http://orcid.org/0000-0002-3988-2659
Emma C. Josefsson http://orcid.org/0000-0001-6478-5204
Marie-Christine Morel-Kopp http://orcid.org/0000-0003-4795-1746
Maggie L. Kalev-Zylinska http://orcid.org/0000-0001-8378-8048

REFERENCES

1. Papadantonakis N, Makitalo M, McCrann DJ, et al. Direct visualization of the endomitotic cell cycle in living megakaryocytes: differential patterns in low and high ploidy cells. Cell Cycle. 2008;7:2352–6.
2. Italiano JE Jr, Lecine P, Shivdasani RA, Hartwig JH. Blood platelets are assembled principally at the ends of proplatelet processes produced by differentiated megakaryocytes. J Cell Biol. 1999;147:1299–312.
3. Dore LC, Crispino JD. Transcription factor networks in erythroid cell and megakaryocyte development. Blood. 2011;118:231–9.
4. Zang C, Luyten A, Chen J, Liu XS, Shivdasani RA. NF-E2, FLI1 and RUNX1 collaborate at areas of dynamic chromatin to activate transcription in mature mouse megakaryocytes. Sci Rep. 2016;6:30255.
5. Kaushansky K. Thrombopoietin: the primary regulator of platelet production. Blood. 1995;86:419–31.
6. Bunting S, Widmer R, Lipari T, et al. Normal platelets and megakaryocytes are produced in vivo in the absence of thrombopoietin. Blood. 1997;90:3423–9.
7. Ito T, Ishida Y, Kashiwagi R, Kuriya S. Recombinant human c-Mpl ligand is not a direct stimulator of proplatelet formation in mature human megakaryocytes. Br J Haematol. 1996;94:387–90.
8. Italiano JE Jr. Unraveling mechanisms that control platelet production. Semin Thromb Hemost. 2013;39:15–24.
9. Poulter NS, Thomas SG. Cytoskeletal regulation of platelet formation: coordination of F-actin and microtubules. Int J Biochem Cell Biol. 2015;66:69–74.
10. Klampfl T, Gisslinger H, Harutyunyan AS, et al. Somatic mutations of calreticulin in myeloproliferative neoplasms. N Engl J Med. 2013;369:2379–90.
11. Nangalia J, Massie CE, Baxter EJ, et al. Somatic CALR mutations in myeloproliferative neoplasms with nonmutated JAK2. N Engl J Med. 2013;369:2391–405.

12. Xu W, Longo FJ, Wintermantel MR, Jiang X, Clark RA, DeLisle S. Calreticulin modulates capacitative Ca2+ influx by controlling the extent of inositol 1,4,5-trisphosphate-induced Ca2+ store depletion. J Biol Chem. 2000;275:36676–82.
13. Vannucchi AM, Rotunno G, Bartalucci N, et al. Calreticulin mutation-specific immunostaining in myeloproliferative neoplasms: pathogenetic insight and diagnostic value. Leukemia. 2014;28:1811–8.
14. Shivarov V, Ivanova M, Tiu RV. Mutated calreticulin retains structurally disordered C terminus that cannot bind Ca(2+): some mechanistic and therapeutic implications. Blood Cancer J. 2014;4:e185.
15. Pietra D, Rumi E, Ferretti VV, et al. Differential clinical effects of different mutation subtypes in CALR-mutant myeloproliferative neoplasms. Leukemia. 2016;30:431–8.
16. Soboloff J, Rothberg BS, Madesh M, Gill DL. STIM proteins: dynamic calcium signal transducers. Nat Rev Mol Cell Biol. 2012;13:549–65.
17. Grosse J, Braun A, Varga-Szabo D, et al. An EF hand mutation in Stim1 causes premature platelet activation and bleeding in mice. J Clin Invest. 2007;117:3540–50.
18. Di Buduo CA, Balduini A, Moccia F. Pathophysiological significance of store-operated calcium entry in megakaryocyte function: opening new paths for understanding the role of calcium in thrombopoiesis. Int J Mol Sci. 2016;17:2055.
19. Lacabaratz-Porret C, Launay S, Corvazier E, Bredoux R, Papp B, Enouf J. Biogenesis of endoplasmic reticulum proteins involved in Ca2+ signalling during megakaryocytic differentiation: an in vitro study. Biochem J. 2000;350(Pt 3):723–34.
20. Sugiyama T, Yamamoto-Hino M, Miyawaki A, Furuichi T, Mikoshiba K, Hasegawa M. Subtypes of inositol 1,4,5-trisphosphate receptor in human hematopoietic cell lines: dynamic aspects of their cell-type specific expression. FEBS Lett. 1994;349:191–6.
21. Ramanathan G, Mannhalter C. Increased expression of transient receptor potential canonical 6 (TRPC6) in differentiating human megakaryocytes. Cell Biol Int. 2016;40:223–31.
22. Mountford JC, Melford SK, Bunce CM, Gibbins J, Watson SP. Collagen or collagen-related peptide cause (Ca2+)i elevation and increased tyrosine phosphorylation in human megakaryocytes. Thromb Haemost. 1999;82:1153–9.
23. Di Buduo CA, Moccia F, Battiston M, et al. The importance of calcium in the regulation of megakaryocyte function. Haematologica. 2014;99:769–78.
24. Mahaut-Smith MP. The unique contribution of ion channels to platelet and megakaryocyte function. J Thromb Haemost. 2012;10:1722–32.
25. den Dekker E, Molin DG, Breikers G, et al. Expression of transient receptor potential mRNA isoforms and Ca(2+) influx in differentiating human stem cells and platelets. Biochim Biophys Acta. 2001;1539:243–55.
26. Ikeda M. Characterization of functional P2X(1) receptors in mouse megakaryocytes. Thromb Res. 2007;119:343–53.
27. Balduini A, Di Buduo CA, Malara A, et al. Constitutively released adenosine diphosphate regulates proplatelet formation by human megakaryocytes. Haematologica. 2012;97:1657–65.
28. Bjorquist A, Di Buduo CA, Femia EA, et al. Studies of the interaction of ticagrelor with the P2Y13 receptor and with P2Y13-dependent pro-platelet formation by human megakaryocytes. Thromb Haemost. 2016;116:1079–88.
29. Schedel A, Thornton S, Schloss P, Kluter H, Bugert P. Human platelets express functional alpha7-nicotinic acetylcholine receptors. Arterioscler Thromb Vasc Biol. 2011;31:928–34.
30. Genever PG, Wilkinson DJ, Patton AJ, et al. Expression of a functional *N*-methyl-D-aspartate -type glutamate receptor by bone marrow megakaryocytes. Blood. 1999;93:2876–83.
31. Hitchcock IS, Skerry TM, Howard MR, Genever PG. NMDA receptor-mediated regulation of human megakaryocytopoiesis. Blood. 2003;102:1254–9.
32. Traynelis SF, Wollmuth LP, McBain CJ, et al. Glutamate receptor ion channels: structure, regulation, and function. Pharmacol Rev. 2010;62:405–96.
33. Kamal T, Green TN, Morel-Kopp MC, et al. Inhibition of glutamate regulated calcium entry into leukemic megakaryoblasts reduces cell proliferation and supports differentiation. Cell Signal. 2015;27:1860–72.
34. Ogura M, Morishima Y, Okumura M, et al. Functional and morphological differentiation induction of a human megakaryoblastic leukemia cell line (MEG-01s) by phorbol diesters. Blood. 1988;72:49–60.
35. Schweinfurth N, Hohmann S, Deuschle M, Lederbogen F, Schloss P. Valproic acid and all trans retinoic acid differentially induce megakaryopoiesis and platelet-like particle formation from the megakaryoblastic cell line MEG-01. Platelets. 2010;21:648–57.
36. Eckly A, Strassel C, Cazenave JP, Lanza F, Leon C, Gachet C. Characterization of megakaryocyte development in the native bone marrow environment. Methods Mol Biol. 2012;788:175–92.
37. Kalev-Zylinska ML, Green TN, Morel-Kopp MC, et al. *N*-methyl-D-aspartate receptors amplify activation and aggregation of human platelets. Thromb Res. 2014;133:837–47.
38. Green TN, Hamilton JR, Morel-Kopp MC, et al. Inhibition of NMDA receptor function with an anti-GluN1-S2 antibody impairs human platelet function and thrombosis. Platelets. 2017;28:799–811.
39. D'Mello SA, Joseph WR, Green TN, et al. Selected GRIN2A mutations in melanoma cause oncogenic effects that can be modulated by extracellular glutamate. Cell Calcium. 2016;60:384–95.
40. McGlashan SR, Haycraft CJ, Jensen CG, Yoder BK, Poole CA. Articular cartilage and growth plate defects are associated with chondrocyte cytoskeletal abnormalities in Tg737orpk mice lacking the primary cilia protein polaris. Matrix Biol. 2007;26:234–46.
41. Lubbert M, Koeffler HP. Myeloid cell lines: tools for studying differentiation of normal and abnormal hematopoietic cells. Blood Rev. 1988;2:121–33.
42. Tingley WG, Ehlers MD, Kameyama K, et al. Characterization of protein kinase A and protein kinase C phosphorylation of the *N*-methyl-D-aspartate receptor NR1 subunit using phosphorylation site-specific antibodies. J Biol Chem. 1997;272:5157–66.
43. Trecul A, Morceau F, Gaigneaux A, Schnekenburger M, Dicato M, Diederich M. Valproic acid regulates erythro-megakaryocytic differentiation through the modulation of transcription factors and microRNA regulatory micro-networks. Biochem Pharmacol. 2014;92:299–311.
44. Tablin F, Castro M, Leven RM. Blood platelet formation in vitro. The role of the cytoskeleton in megakaryocyte fragmentation. J Cell Sci. 1990;97(Pt 1):59–70.
45. Furuyashiki T, Arakawa Y, Takemoto-Kimura S, Bito H, Narumiya S. Multiple spatiotemporal modes of actin reorganization by NMDA receptors and voltage-gated Ca2+ channels. Proc Natl Acad Sci USA. 2002;99:14458–63.
46. Merriam EB, Lumbard DC, Viesselmann C, et al. Dynamic microtubules promote synaptic NMDA receptor-dependent spine enlargement. PLoS ONE. 2011;6:e27688.
47. Mattison HA, Popovkina D, Kao JP, Thompson SM. The role of glutamate in the morphological and physiological development of dendritic spines. Eur J Neurosci. 2014;39:1761–70.
48. Shirao T, Gonzalez-Billault C. Actin filaments and microtubules in dendritic spines. J Neurochem. 2013;126:155–64.
49. Giardino L, Armelloni S, Corbelli A, et al. Podocyte glutamatergic signaling contributes to the function of the glomerular filtration barrier. J Am Soc Nephrol. 2009;20:1929–40.
50. Schwartz N, Schohl A, Ruthazer ES. Neural activity regulates synaptic properties and dendritic structure in vivo through calcineurin/NFAT signaling. Neuron. 2009;62:655–69.
51. Zaslavsky A, Chou ST, Schadler K, et al. The calcineurin-NFAT pathway negatively regulates megakaryopoiesis. Blood. 2013;121:3205–15.

52. Thompson CJ, Schilling T, Howard MR, Genever PG. SNARE-dependent glutamate release in megakaryocytes. Exp Hematol. 2010;38:504–15.
53. Bhangu PS, Genever PG, Spencer GJ, Grewal TS, Skerry TM. Evidence for targeted vesicular glutamate exocytosis in osteoblasts. Bone. 2001;29:16–23.
54. Prevarskaya N, Ouadid-Ahidouch H, Skryma R, Shuba Y. Remodelling of Ca2+ transport in cancer: how it contributes to cancer hallmarks? Philos Trans R Soc Lond B Biol Sci. 2014;369:20130097.
55. Monteith GR, Prevarskaya N, Roberts-Thomson SJ. The calcium-cancer signalling nexus. Nat Rev Cancer. 2017;17:367–80.

SUPPORTING INFORMATION

Additional Supporting Information may be found online in the supporting information tab for this article.

How to cite this article: Kamal T, Green TN, Hearn JI, et al. *N*-methyl-D-aspartate receptor mediated calcium influx supports in vitro differentiation of normal mouse megakaryocytes but proliferation of leukemic cell lines. *Res Pract Thromb Haemost*. 2018;2:125–138. https://doi.org/10.1002/rth2.12068

Author/s:
Kamal, T; Green, TN; Hearn, J; Josefsson, EC; Morel-Kopp, M-C; Ward, CM; During, MJ; Kalev-Zylinska, ML

Title:
N-methyl-D-aspartate receptor mediated calcium influx supports in vitro differentiation of normal mouse megakaryocytes but proliferation of leukemic cell lines

Date:
2018-01-01

Citation:
Kamal, T., Green, T. N., Hearn, J., Josefsson, E. C., Morel-Kopp, M. -C., Ward, C. M., During, M. J. & Kalev-Zylinska, M. L. (2018). N-methyl-D-aspartate receptor mediated calcium influx supports in vitro differentiation of normal mouse megakaryocytes but proliferation of leukemic cell lines. RESEARCH AND PRACTICE IN THROMBOSIS AND HAEMOSTASIS, 2 (1), pp.125-138. https://doi.org/10.1002/rth2.12068.

Persistent Link:
http://hdl.handle.net/11343/270881

File Description:
Published version